Available online at www.sciencedirect.com

ScienceDirect

Energy Procedia 81 (2015) 11 – 21

Energy Procedia

69th Conference of the Italian Thermal Engineering Association, ATI 2014

On the Influence of Geometrical Features and Wind Direction over an Urban Canyon Applying a FEM Analysis

Gabriele Battista[a,]*, Luca Evangelisti[a], Claudia Guattari[a], Roberto De Lieto Vollaro[a]

[a]*University of Roma TRE, Department of engineering, via Vito Volterra 62, Rome – 00146 Italy*

Abstract

The urban areas discomfort is related to the increase of local temperatures due to the geometrical characteristics and thermal properties of the built environment. This study shows the results of a FEM analysis through which a urban canyon geometry has been modelled. A 3D domain has been considered taking into account three different wind directions and to geometrical parameters variation, such as the aspect ratio (Height- Width) and the urban canyon length.

Peer-review under responsibility of the Scientific Committee of ATI 2014

Keywords: Urban canyon, FEM, Simulation, Parameters variation, Wind direction.

1. Introduction

The urban areas discomfort is related to the increase of local temperatures due to the geometrical and thermal characteristics of the built environment. It is well known that some geometrical parameters influence the thermal conditions inside urban areas [1] and one of the main effects of current built environments is the so-called "urban heat island" [2]. This phenomenon can be related to the road geometrical characteristics, building façades features and, finally, to the lack of wide-open spaces [3]. Urbanization has led to an increase of the heat island effect, due to the reduction of green areas in urban environment [4]. The built environment influences buildings energy performance [5-22], dynamic characteristics and thermal properties of air masses, which are related to the quantity, size and distance of buildings. An urban canyon is a place where the street is flanked by buildings on both sides creating a canyon-like

* Corresponding author. Tel.: +39-06-5733-3289.
E-mail address: gabriele.battista@uniroma3.it

Peer-review under responsibility of the Scientific Committee of ATI 2014
doi:10.1016/j.egypro.2015.12.054

environment. Such an environment has an impact on various local conditions: temperature, wind and air quality. Low natural ventilation caused by structures leads to a superheating phenomenon, which facilitates disadvantages during the summer [23].

Ideally a street canyon is a relatively narrow street with tall, continuous buildings on both sides of the road. But now the term urban canyon is used more broadly and the geometrical details of the street canyon are used to categorize them.

The environmental conditions in urban areas can be analysed through a model described by a road and two buildings, one in front of the other. This model is well described by some geometrical characteristics:

- the building height (H);
- the road width (W);
- the road length (L).

Through these parameters an urban canyon classification becomes possible. The most important geometrical detail about a street canyon is the ratio of the canyon height (H) to canyon width (W), H/W, which is defined as the aspect ratio, different H/W ratios strongly influence air quality and environmental conditions. The value of the aspect ratio can be used to classify street canyons as follows:

- Regular canyon - aspect ratio ≈ 1;
- Avenue canyon - aspect ratio < 0.5;
- Deep canyon - aspect ratio ≈ 2.

A sub-classification of each of the above can be done depending on the distance between two major intersections along the street, defined as the length (L) of the street canyon:

- Short canyon - L/H ≈ 3;
- Medium canyon - L/H ≈ 5;
- Long canyon - L/H ≈ 7.

Nomenclature

ρ	Density [kg/m^3]
u	velocity [m/s]
p	Pressure [Pa]
μ	Dynamic viscosity [Pa s]
F	Volume force [N/m^3]
C_p	Specific heat capacity at constant pressure [J/kgK]
T	Temperature [K]
K_v	Thermal conductivity [W/mK]
k	Turbolence kinetic energy [m^2/s^2]
ε	Turbolence dissipation rate [m^2/s^3]
μ_T	Turbolence viscosity [Pa s]
z_0	Aerodynamic roughness length [m]
k_S	Sand-grain roughness height [m]
C_s	Roughness constant
T_a	Ait temperature for validation [K]
T_f	Ground temperature for validation [K]
u_0	Wind velocity for validation [m/s]

During the last years many studies have been conducted on different geometrical configurations of urban canyons and their influence on the local conditions, in terms of pollution, temperature increase and, more in general, environmental conditions [24-29].

In our study a 3D model of an urban canyon has been realized and several simulations have been performed applying a FEM analysis, investigating the influence of different H/W ratio, length and wind direction variations on the environmental conditions.

2. Numerical model

The simulations have been performed under steady state conditions with Reynolds-averaged Navier–Stokes (RANS) equations according to the k–ε standard model. The governing equations are described below [30].

Conservation of momentum:

$$\rho \boldsymbol{u} \cdot \nabla \boldsymbol{u} = -\nabla p + \nabla \cdot \left[\mu \left(\nabla \boldsymbol{u} + \left(\nabla \boldsymbol{u} \right)^T \right) - \frac{2}{3} \mu \left(\nabla \cdot \boldsymbol{u} \right) \boldsymbol{I} \right] + \boldsymbol{F} \tag{1}$$

Conservation of mass:

$$\nabla \cdot \left(\rho \boldsymbol{u} \right) = 0 \tag{2}$$

Conservation of energy:

$$\rho C_p \boldsymbol{u} \cdot \nabla T = \nabla \cdot \left(k_v \cdot \nabla T \right) \tag{3}$$

where u is the averaged air velocity, ρ is the air mass density, μ is the air dynamic viscosity, I is the unitary tensor, F is the volume force vector, p is the air pressure, C_p is the specific heat capacity at constant pressure, T is the air temperature, k_v is the thermal conductivity.

The k-ε model introduces two additional transport equations and two dependent variables: the turbulent kinetic energy k, and the turbulent dissipation rate, ε. The turbulent viscosity is modeled as

$$\mu_T = \rho C_\mu \frac{k^2}{\varepsilon} \tag{4}$$

where C_μ is a model constant. The transport equation for k reads:

$$\rho \boldsymbol{u} \cdot \nabla k = \nabla \cdot \left[\left(\mu + \frac{\mu_T}{\sigma_k} \right) \nabla k \right] + P_k - \rho \varepsilon \tag{5}$$

where the production term is

$$P_k = \mu_T \left(\nabla \boldsymbol{u} : \left(\nabla \boldsymbol{u} + \left(\nabla \boldsymbol{u} \right)^T \right) - \frac{2}{3} \left(\nabla \cdot \boldsymbol{u} \right)^2 \right) - \frac{2}{3} \rho k \nabla \cdot \boldsymbol{u} \tag{6}$$

The operation ":" denotes a contraction between tensors defined by:

$$\boldsymbol{a}:\boldsymbol{b}=\sum_{n}\sum_{m}a_{nm}b_{nm} \tag{7}$$

The transport equation for ε reads:

$$\rho\boldsymbol{u}\cdot\nabla\varepsilon=\nabla\cdot\left[\left(\mu+\frac{\mu_T}{\sigma_\varepsilon}\right)\nabla\varepsilon\right]+C_{\varepsilon1}P_k\frac{\varepsilon}{k}-C_{\varepsilon2}\rho\frac{\varepsilon^2}{k} \tag{8}$$

where the C_μ, $C_{\varepsilon1}$, $C_{\varepsilon2}$, σ_k, σ_ε are constants determined from experimental data [31].

Furthermore, the implemented CFD model is described by geometrical features. Regarding the urban canyon taken into account, three different H/W ratio values (equal to 0.5, 1 and 4) and three different road length values (equal to 60, 100 and 140 m) were considered. All geometrical models are characterized by buildings width and height equal to 20 m. Tominaga [32] wrote a guideline for the CFD use in which the computational domain dimensions were chosen in relation to the buildings height (H), as shown in Fig. 1.

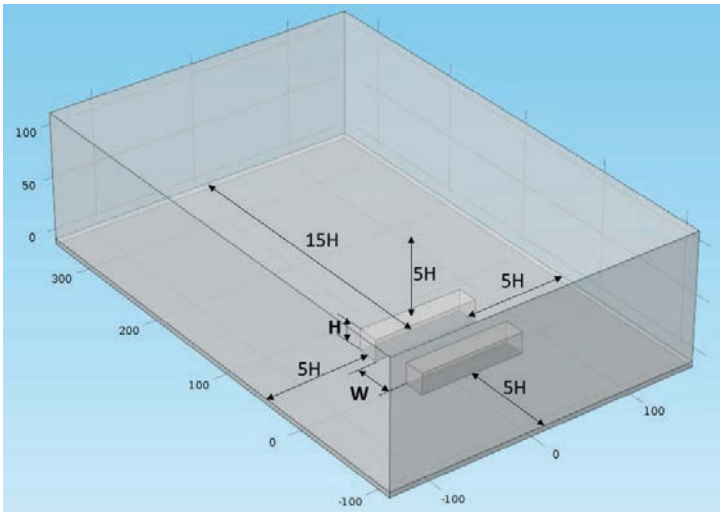

Fig. 1. 3D computational domain dimensions.

To simulate the ground influence, the computational domain has been extended for 5m under this one.
The materials properties used in the model are listed in Table 1.

Table 1. Materials properties.

Element	Mass density (kg/m3)	Specific heat capacity (J/kgK)	Thermal conductivity (W/mK)	Temperature at -5m (K)	Temperature (K)	Velocity (m/s)
Ground	1000	1000	2	288.15	-	-
Buildings wall	1000	1000	0.15	-	-	-
Undisturbed air	-	-	-	-	303.15	2

The ground roughness values (e.g. the sand-grain roughness height k_s (m) and the roughness constant C_s), were determined using the consistency relationship with the aerodynamic roughness length z_0 derived by Blocken [33]. The values selected for this study are k_s = 1m and C_s = 0.5. Regarding the building façades, no specific roughness was

considered. The resulting z_0 value (Eq. (9)) is 0.05 m. It has been considered that this value properly represents the outer region roughness.

$$k_S = \frac{9.793 \cdot z_0}{C_S} \tag{9}$$

The initial values implemented in the computational domain are the outcomes of several simulations, whose are the results of the solver convergence phase. The initial values were set equal to 79°C for the solid domain, 30°C for the fluid domain, and the turbulent kinetic energy and the turbulent dissipation rate were set equal to zero.

The mesh of the model is composed by tetrahedral cells. The mesh is more dense near the ground and around the buildings to better describe the urban canyon. Considering the canyon geometry characterized by a H/W ratio equal to 1 and a canyon length equal to 100m, the average mesh quality is about 0.7471. The mesh quality provides the geometrical distortion of a cell through the spatial difference between the cell nodes (for instance an “ideal” 2D cell is characterized by an equilateral triangle or a square). It is worth to notice that the given mesh quality value is good for a fluid dynamic computational model. The number of cells implemented in the simulation comes from many simulations carried out in order to achieve the convergence in the middle of the canyon for both velocity and temperature profile.

3. CFD model Validation

The numerical model validation was assessed through the comparison with the wind tunnel experiment performed by Uehara [34]. In this study the numerical validation test, considering H/W = 1 and L = 100m, was carried out. The air temperature T_a was set equal to 20°C (293.15 K); the ground temperature T_f was set equal to 79°C (352.15 K), the inflow wind speed u_0, perpendicular to the buildings façades, was set equal to 1.5 m/s, in order to reproduce the experimental tests conditions. The comparison between the data obtained by means of wind tunnel experiments and numerical test are shown in Fig. 2, where the simulated data are referred to the mean value related to the vertical lines in the center of the canyon. In Fig. 2a the vertical profile of the normalized horizontal velocity u/u_0 is shown, in Fig. 2b the vertical profile of normalized temperature $(T\text{-}T_f)/(T_a\text{-}T_f)$ is illustrated. As Lei [35] shows, the agreement between the numerical model and the wind tunnel experiment is good, although the numerical model overestimates the wind speed and temperature values.

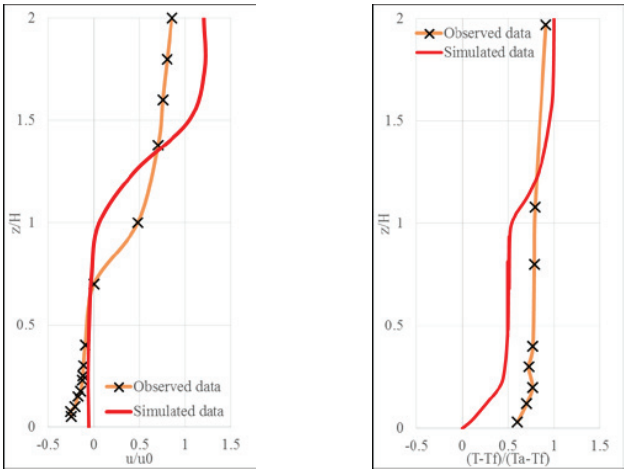

(a) (b)

Fig. 2. Comparison between the simulated data and the observed data by Uehara (2000) [34]. (a) vertical profile of normalized horizontal velocity u/u_0, where u_0 is the reference horizontal wind speed; (b) normalized vertical profile temperature $(T\text{-}T_f)/(T_a\text{-}T_f)$ along the center line of the street canyon, where T_f and T_a are the ground temperature and the air inlet temperature, respectively.

4. Results and Discussion

In order to evaluate the effect of the geometrical parameters H/W and L/H variation on the street canyon climate conditions, a comparison between several steady-state simulations was performed. As it can be seen in Table 2, each case study is characterized by an H/W value and for each aspect ratio three different canyon lengths have been considered (L=60 m, L=100 m, L=140 m). In order to investigate the wind effect on the different canyon geometrical configurations three canyon orientations have been taken into account (Fig.3).

Table 2. Case studies conditions.

H/W	0.5	1	4
	Canyon Orientation		
L = 60 m	0°, 45°, 90°	0°, 45°, 90°	0°, 45°, 90°
L = 100 m	0°, 45°, 90°	0°, 45°, 90°	0°, 45°, 90°
L = 140 m	0°, 45°, 90°	0°, 45°, 90°	0°, 45°, 90°

The wind effect on buildings, for each case study, is described by a laminar air flow characterized by a velocity equal to 2 m/s and a temperature equal to 30°C (303.15 K).

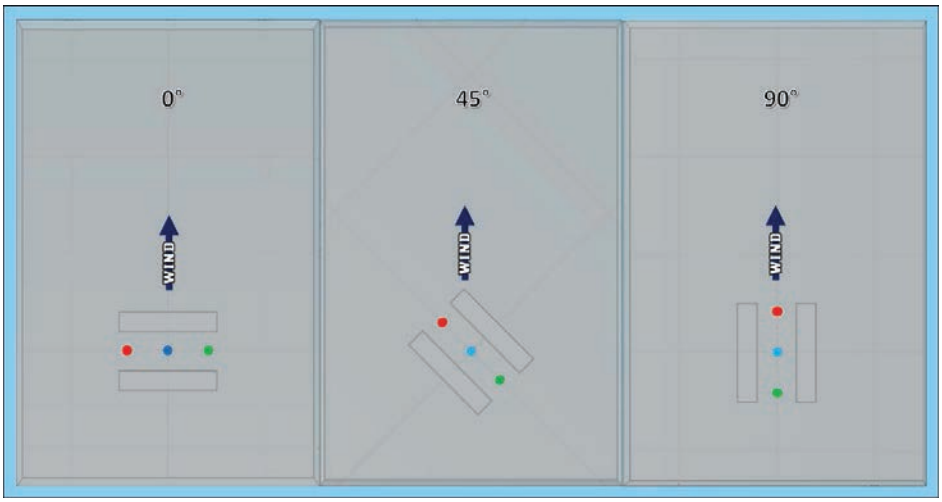

Fig. 3. Analyzed canyon orientations.

Fig. 3 shows the canyon orientation taken into account and the three vertical lines (each 20m high), placed on the road axis, over which measurements have been performed.

Fig. 4 shows for different canyon geometrical characteristics taken into account the results related to the 0° orientation. The abscissa axis shows the air velocity values and the ordinate axis shows the z/H ratio, where z is the height above the road level. It is possible to observe the same trend for the aspect ratio equal to 1 and 4 in which the velocity values are very low, ranging between 0.1 and 0.5 m/s, velocity values higher than these are shown only for z/H bigger than 0.9. Only for the canyons characterized by H/W equal to 0.5, for each length, the vertical velocity variation for each measurements line is higher than the other cases. Moreover, it is worth to notice that air velocity can reach values equal to 1 m/s also for low z/H ratios. This could be expected because the distance between buildings façades is very large and this leads to a major turbulence.

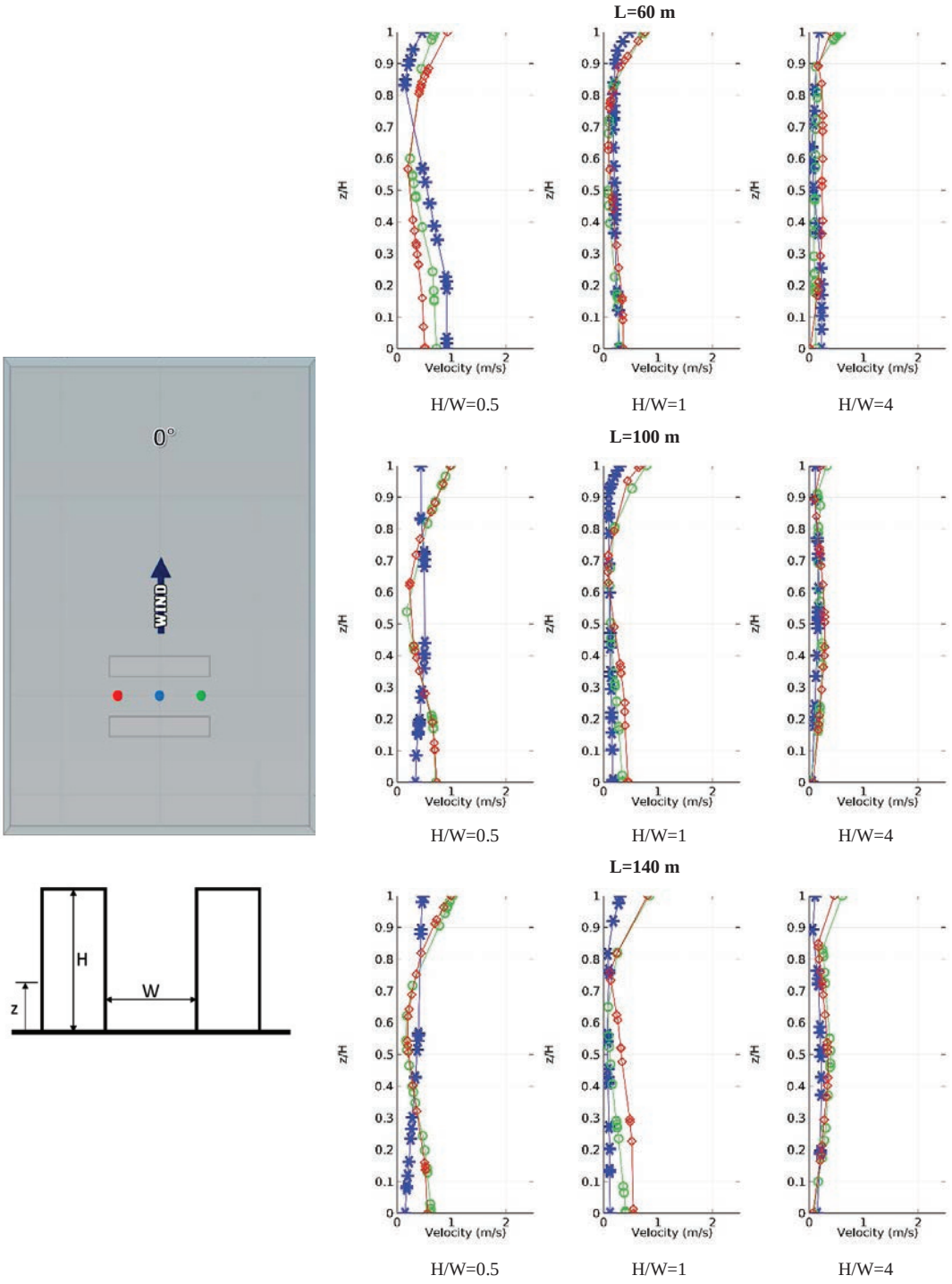

Fig. 4. Vertical velocity profile referred to a canyon orientation equal to 0°. The blue line is placed in the middle of the canyon, the green and the red lines are placed at 10 m from the two openings (see Fig.3).

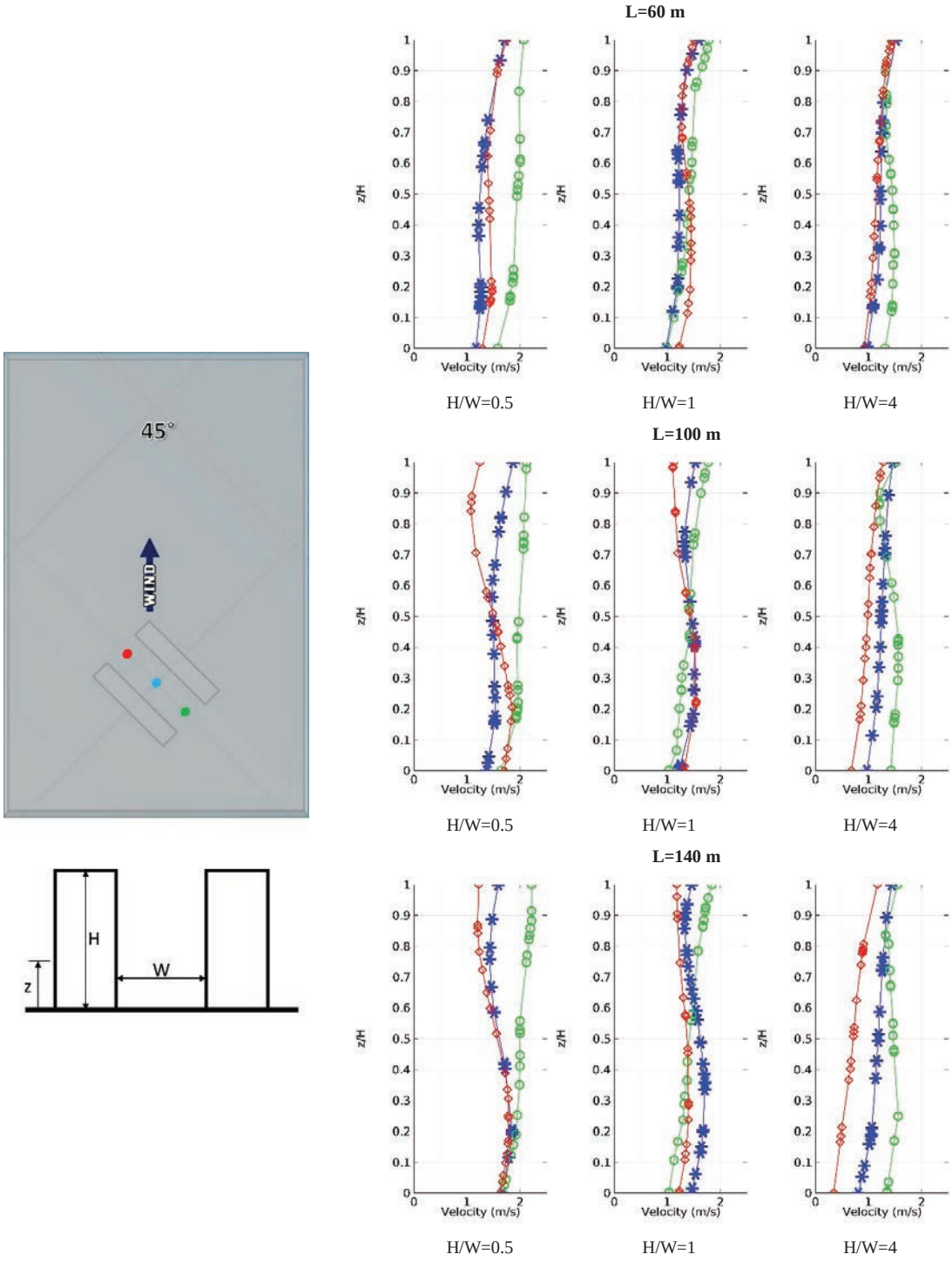

Fig. 5. Vertical velocity profile referred to a canyon orientation equal to 45°. The blue line is placed in the middle of the canyon, the green and the red lines are placed at 10 m from the two openings (see Fig.3).

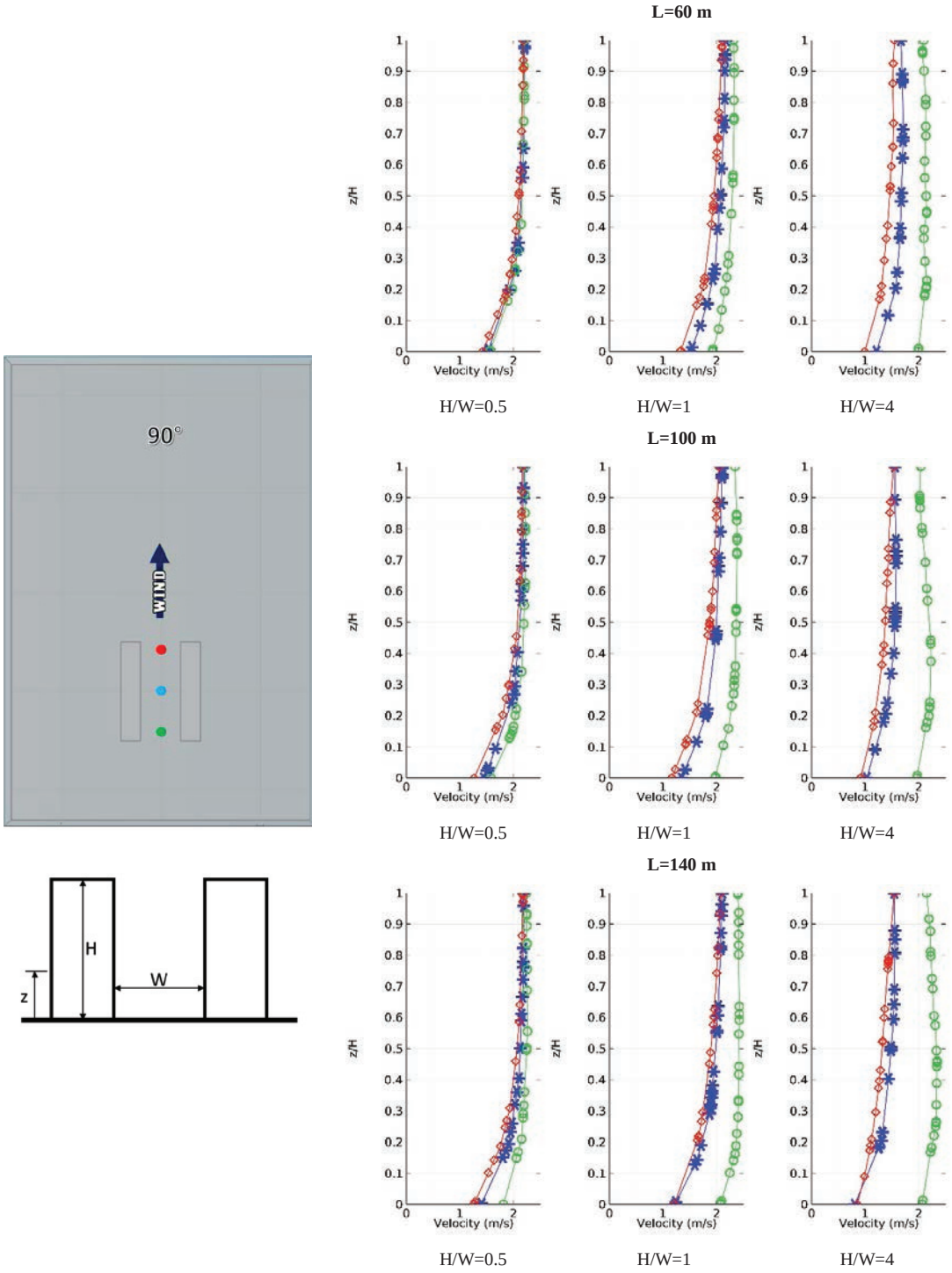

Fig. 6. Vertical velocity profile referred to a canyon orientation equal to 90°. The blue line is placed in the middle of the canyon, the green and the red lines are placed at 10 m from the two openings (see Fig.3).

Fig. 5 shows the result related to the 45° orientation. These cases are characterized by a higher air velocity variation along z than the previous case. It is possible to notice that, when the H/W is equal to 4, the canyon length increase causes significant velocity variation along the three different measurement lines from 0.3 to 1.5 m/s. Canyons characterized by an aspect ratio equal to 1 show the same trend, air velocity values ranging from 1 to 1.5 m/s. Finally, canyons characterized by an aspect ratio equal to 0.5 show air velocity values ranging from 1 to 2 m/s and the largest air velocity variations occur for high z/H values, despite what happen for H/W = 4 where these changes are inverted.

Fig. 6 shows the result related to the 90° orientation. In these cases when H/W is equal to 0.5 the trend is equal along each measurements line. Instead, when H/W value increases the air velocity variations increase too. Indeed, for aspect ratio equal to 4, the vertical velocity values ranging from 0.7 to 2.5 m/s. All these results are strongly independent from canyon length.

Considering the whole set of data, for the same canyon length, it is worth to notice that air velocity values significantly increase for the canyon orientation move from 0° to 90°.

5. Conclusions

In this study several numerical simulations of different urban canyon configurations in a 3D domain have been carried out. The simulated scenarios have been performed under steady-state condition along three vertical measurement lines, by taking into account different H/W ratio values, canyon lengths and wind directions. These different features aim at investigating the relationships between the urban canyon configuration and the wind direction.

The results points out that the air velocity values are independent from the canyon length. When the wind direction changes the air velocity values increase, moving from about 0 m/s to 2.5 m/s, in spite of an air inflow velocity equal to 2 m/s. When the wind direction is not perpendicular to the buildings façades the air velocity values are high with a subsequent advantage in terms of air pollutions: the canalized air flows allow a pollution agents decrease.

Future developments of this research, currently under investigation, aim to analyze asymmetric canyon configurations where buildings that make the canyon have significant height differences. The research group is also studying the relationship between the urban canyon and the surrounding built environments.

References

[1] Lien F.S., Yee E., Cheng Y. Simulation of mean flow and turbulence over a 2D building array using high-resolution CFD and a distributed drag force approach. Wind Engineering and Industrial Aerodynamics 2004; 92: 117-158.

[2] Memon R.A., Leung D.Y.C., Liu C. An investigation of urban heat island intensity (UHII) as an indicator of urban heating. Atmospheric Research 2009; 94: 491–500.

[3] Gago E.J., Roldan J., Pacheco-Torres R., Ordóñez J. The city and urban heat islands: A review of strategies to mitigate adverse effects. Renewable and Sustainable Energy Reviews 2013; 25: 749-758.

[4] Cui L., Shi J. Urbanization and its environmental effects in Shanghai, China. Urban Climate 2012; 2: 1-15.

[5] Battista G., Evangelisti L., Guattari C., Basilicata C., De Lieto Vollaro R. Buildings Energy Efficiency: Interventions Analysis under a Smart Cities Approach. Sustainability 2014; 6: 4694-4705.

[6] Evangelisti L., Battista G., Guattari C., Basilicata C., De Lieto Vollaro R. Influence of the Thermal Inertia in the European Simplified Procedures for the Assessment of Buildings' Energy Performance. Sustainability 2014; 6: 4514-4524.

[7] Evangelisti L., Battista G., Guattari C., Basilicata C., De Lieto Vollaro R. Analysis of Two Models for Evaluating Energy Performance of Different Buildings. Sustainability 2014; 6: 5311-5321.

[8] De Lieto Vollaro R., Evangelisti L., Battista G., Gori P., Guattari C., Fanchiotti A. Bus for Urban Public Transport: Energy Performance Optimization. Energy Procedia 2014; 45: 731-738.

[9] De Lieto Vollaro R., Evangelisti L., Carnielo E., Battista G., Gori P., Guattari C., Fanchiotti A. An integrated approach for an historical buildings energy analysis in a smart cities perspective. Energy Procedia 2014; 45: 372-378.

[10] De Lieto Vollaro R., Calvesi M., Battista G., Evangelisti L., Botta F. Calculation model for optimization design of low impact energy systems for buildings. Energy Procedia 2014; 48: 1459-1467.

[11] De Lieto Vollaro R., Guattari C., Evangelisti L., Battista G., Carnielo E., Gori P. Building energy performance analysis: A case study. Energy and Buildings 2015; 87: 87-94.

[12] Battista G., Carnielo E., Evangelisti L., Frascarolo M., De Lieto Vollaro R. Energy performances and thermal comfort of an high efficiency house: RhOME for denCity, winner of Solar Decathlon Europe 2014. Sustainability 2015; 7: 9681-9695.

[13] Peruzzi L., Salata F., De Lieto Vollaro A., De Lieto Vollaro R. The reliability of technological systems with high energy efficiency in residential buildings. Energy and Buildings 2014; 68: 19-24.

[14] Zinzi M., Carnielo E., Federici A. Preliminary studies of a cool roofs' energy-rating system in Italy. Advances in Building Energy Research 2014; 8 (1): 84-96
[15] Zinzi M., Carnielo E., Agnoli S. Characterization and assessment of cool coloured solar protection devices for Mediterranean residential buildings application. Energy and Buildings 2012; 50: 111-119
[16] Carnielo E.; Zinzi M. Optical and thermal characterisation of cool asphalts to mitigate urban temperatures and building cooling demand. Building and Environment 2013; 60: 56-65
[17] Salata F., De Lieto Vollaro A., De Lieto Vollaro R., Davoli M. Plant reliability in hospital facilities. Energy Procedia 2014; 45: 1195-1204
[18] Coppi M., Quintino A., Salata F. Numerical study of a vertical channel heated from below to enhance natural ventilation in a residential building. International Journal of Ventilation 2013; 12 (1): 41-49.
[19] Salata F., De Lieto Vollaro A., De Lieto Vollaro R., Mancieri L. Method for energy optimization with reliability analysis of a trigeneration and teleheating system on urban scale: a case study. Energy and Buildings 2015; 86: 118–136.
[20] Salata F., Golasi I., De Lieto Vollaro A., De Lieto Vollaro R. How high albedo and traditional buildings' materials and vegetation affect the quality of urban microclimate. A case study. Energy and Buildings 2015; 99: 32-49.
[21] Salata F., De Lieto Vollaro A., De Lieto Vollaro R. A case study of technical and economic comparison among energy production systems in a complex of historic buildings in Rome. Energy Procedia 2014; 45: 482-491.
[22] Galli G., Vallati A., Recchiuti C., de Lieto Vollaro R., Botta, F. Passive cooling design options to improve thermal comfort in an Urban District of Rome, under hot summer conditions. International Journal of Engineering and Technology 2013; 5(5): 4495-4500.
[23] Latini, G., Passerini G. Local climate: Climatology and Biometeorology in urban areas (in Italian: Il clima locale: Climatologia e Biometeorologia delle aree urbane). BIOARCHITETTURA 2006; 50-51-52.
[24] Takebayashi H., Moriyama M. Relationships between the properties of an urban street canyon and its radiant environment: Introduction of appropriate urban heat island mitigation technologies. Solar Energy 2012; 86 (9): 2255-2262.
[25] Xie X., Liu C.H., Leung D.Y.C. Impact of building facades and ground heating on wind flow and pollutant transport in street canyons. Atmospheric Environment 2007; 41 (39): 9030–9049.
[26] De Lieto Vollaro R., Vallati A., Bottillo S. Differents Methods to Estimate the Mean Radiant Temperature in an Urban Canyon. Advances in Materials Science and Engineering 2013; 650: 647-651.
[27] Bottillo S., De Lieto Vollaro A., Galli G,; Vallati A. CFD modeling of the impact of solar radiation in a tridimensional urban canyon at different wind conditions. Solar Energy 2014; 102: 212-222.
[28] Bottillo S., De Lieto Vollaro A., Galli G., Vallati A. Fluid dynamic and heat transfer parameters in an urban canyon. Solar Energy 2014; 99: 1-10.
[29] De Lieto Vollaro A., de Simone G., Romagnoli R., Vallati A., Bottillo S. Numerical Study of Urban Canyon Microclimate Related to Geometrical Parameters. Sustainability 2014; 6(11): 7894-7905.
[30] Batchelor G.K. An Introduction To Fluid Dynamics. Cambridge University Press 1967.
[31] Wilcox D.C. Turbulence Modeling for CFD. DCW Industries 2nd edition 1998.
[32] Tominaga Y., Mochida A., Yoshie R., Kataoka H., Nozu T., Yoshikawa M., Shirasawa T. AIJ guidelines for practical applications of CFD to pedestrian wind environment around buildings. Wind Engineering and Industrial Aerodynamics 2008; 96: 1749-1761.
[33] Blocken B., Stathopoulos T., Carmeliet J. CFD simulation of the atmospheric boundary layer: wall function problems. Atmospheric Environment 2007; 41 (2): 238-252.
[34] Uehara K., Murakami S., Oikawa S., Wakamatsu S. Wind tunnel experiments on how thermal stratification affects flow in and above urban street canyons. Atmospheric Environment 2000; 34 (10): 1553-1562.
[35] Lei L., Lin Y., Li-Jie Z., Yin J. Numerical study on the impact of ground heating and ambient wind speed on flow fields in street canyons. Advances in Atmospheric Sciences 2012; 29 (6): 1227–1237.